Supplementary Information

# Potentiating hypoxic microenvironment for antibiotic activation by photodynamic therapy to combat bacterial biofilm infections

Weijun Xiu[1], Ling Wan[1], Kaili Yang[1], Xiao Li[1], Lihui Yuwen[1,*], Heng Dong[2], Yongbin Mou[2], Dongliang Yang[3], and Lianhui Wang[1,*]

[1]State Key Laboratory for Organic Electronics and Information Displays & Jiangsu Key Laboratory for Biosensors, Institute of Advanced Materials (IAM), Jiangsu National Synergetic Innovation Centre for Advanced Materials (SICAM), Nanjing University of Posts and Telecommunications, Nanjing 210023, China

[2]Nanjing Stomatological Hospital, School of Medicine, Nanjing University, Nanjing, 210008, China

[3]School of Physical and Mathematical Sciences & Institute of Advanced Materials (IAM), Nanjing Tech University, Nanjing 211800, China

[*]Correspondence and requests for materials should be addressed to L. Y. (email: iamlhyuwen@njupt.edu.cn) and L. W. (email: iamlhwang@njupt.edu.cn).

## Supplementary Methods

***In vitro*** **antibacterial activity of MNZ under different oxygen levels.** Methicillin-resistant *Staphylococcus aureus* (MRSA, ATCC43300) were grown in chemically defined medium under shaking at 220 rpm and 37°C over 12 h and further diluted to $10^7$ CFU/mL with chemically defined medium[1]. The MRSA suspension was mixed with different concentrations of MNZ and incubated under different oxygen levels. The antibacterial efficiency of MNZ was evaluated by using plate counting method.

**Penetration of MNZ in MRSA biofilms.** Firstly**,** the MRSA biofilm was growth in Transwell inserts for 48 h. Then, PBS dispersions of HCM NPs (Ce6: 50 μg/mL, MNZ: 25 μg/mL) were transferred into the inserts and incubated with MRSA biofilms for different times, and irradiated with 635 nm laser (20 mW/cm$^2$, 30 min) for PDT group. The amount of MNZ penetrated into receiver plate was calculated by using UV-vis absorption spectroscopy (UV-3600, Shimadzu, Japan).

**Quantitative real-time PCR.** The RNA was extracted from MRSA under different experimental conditions by using bacteria total RNA isolation kit (Sangon Biotech, China). The complementary DNA (cDNA) was further synthesized by using a reverse transcription kit (Takara) as per the instructions. The expression levels of genes encoding fibronectin binding protein B (*fnbB*), elastin binding protein (*ebps*), and intercellular adhesion biofilm required genes type C and D (*icaC and icaD*) were detected by using the synergy brands (SYBR) Green Select Master Mix (Bio-Rad) in triplicate on an AbiPrism 7900 HT cycler (Applied Biosystems), with 16sRNA as a normalized gene. The fold change of the target mRNA relative to the controls was determined using the $2^{-\Delta\Delta CT}$ method. All primers used in qPCR were designed according to previous report and were listed in Supplementary Table 1[2].

**Wound blotting for MRSA biofilm detection.** The nitrocellulose membrane was pressed to the infected tissues of mice for 10 seconds and left for natural drying. After stained with ruthenium red (5 mg/mL) for 1 min, the membrane was washed three times by soaking in a mixed solution (containing 40% methanol 10% acetic acid) for 30 minutes to decrease the amount of nonspecifically bound staining solution[3]. The stained membrane was then photographed.

## Supplementary Figures

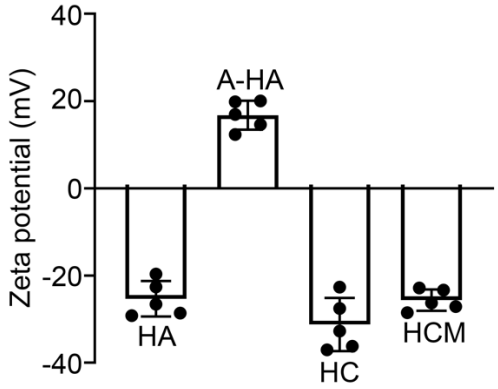


**Supplementary Fig. 1** Zeta potential of HA, A-HA, HC NPs, and HCM NPs (n = 5 independent samples; mean ± SD). Source data are provided as a Source Data file.

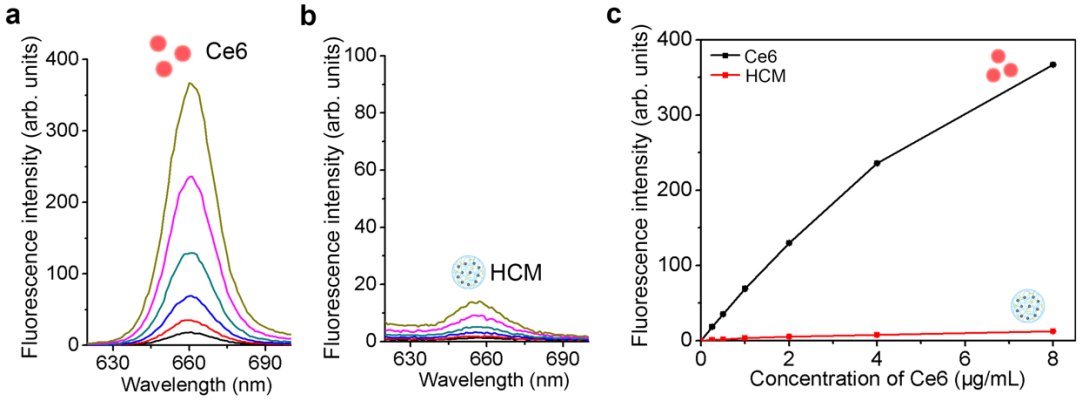


**Supplementary Fig. 2** Aggregation induced fluorescence quenching of Ce6 in HCM NPs. **a,b,** Fluorescence intensity of Ce6 (**a**) and HCM NPs (**b**) at different concentrations (from bottom to top, Ce6: 0.2, 0.5, 1, 2, 4, 8 μg/mL). **c,** Fluorescence intensity of Ce6 and HCM NPs dispersions at different concentrations. Source data are provided as a Source Data file.

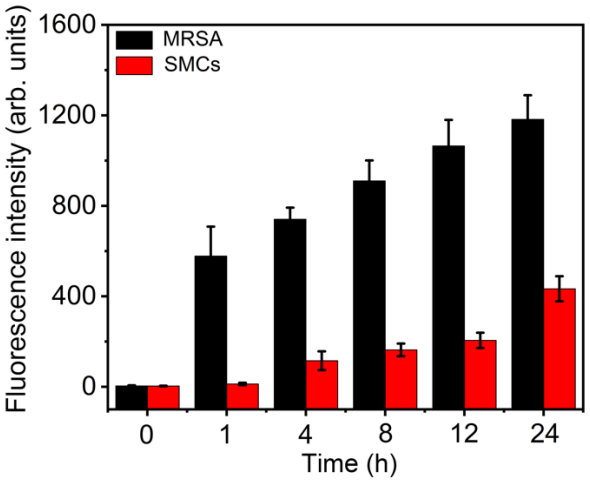


**Supplementary Fig. 3** Fluorescence intensity of HCM NPs solutions (Ce6: 20 μg/mL) after incubated with MRSA biofilms and mice smooth muscle cells (SMCs) for different times (n = 20 biologically independent samples; mean ± SD). Source data are provided as a Source Data file.

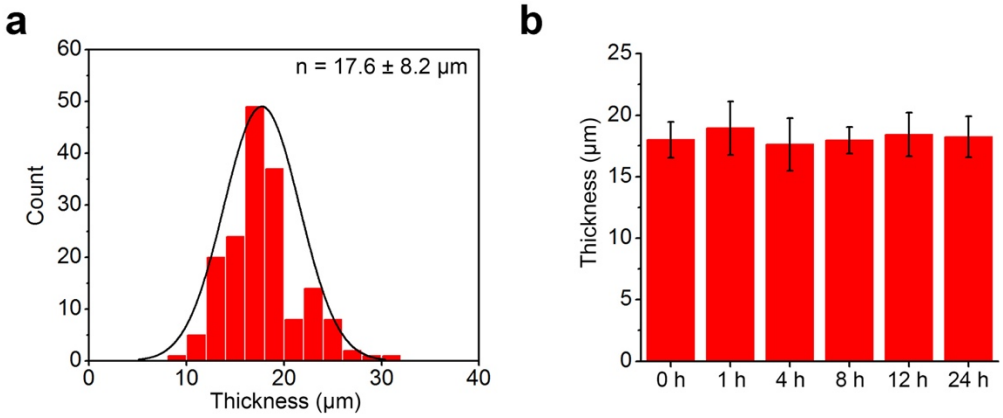


**Supplementary Fig. 4** Thickness of MRSA biofilms. **a,** Thickness of MRSA biofilms without any treatment (n=200). **b,** Thickness of MRSA biofilms after incubation with HCM NPs for different times (n = 20 biologically independent samples; mean ± SD). Source data are provided as a Source Data file.

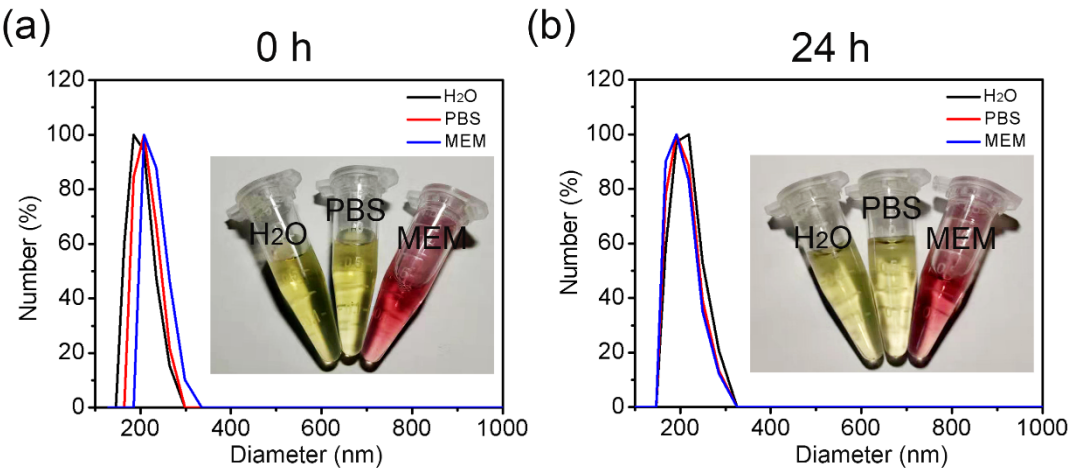


**Supplementary Fig. 5** Colloidal stability of HCM NPs. **a,b,** Hydrodynamic sizes and photographs (inset) of HCM NPs (Ce6: 20 μg/mL; MNZ: 10 μg/mL) dispersed in different mediums ($H_2O$, PBS, and minimum Eagle's medium (MEM)) for 0 h (**a**) and 24 h (**b**). Source data are provided as a Source Data file.

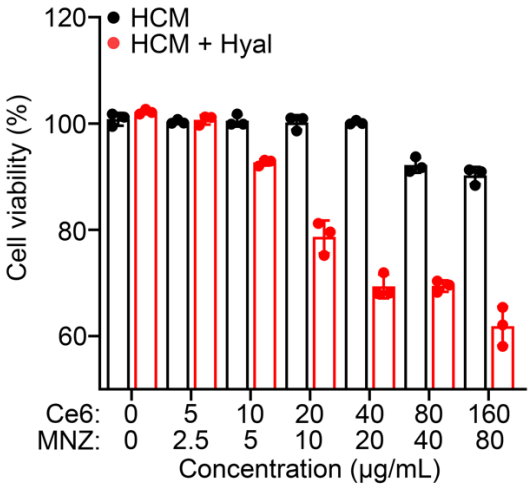


**Supplementary Fig. 6** Viability of human normal liver (L-O2) cells incubated with HCM NPs or HCM NPs + Hyal (100 unit/mL) for 24 h (n = 3 biologically independent samples; mean ± SD). Source data are provided as a Source Data file.

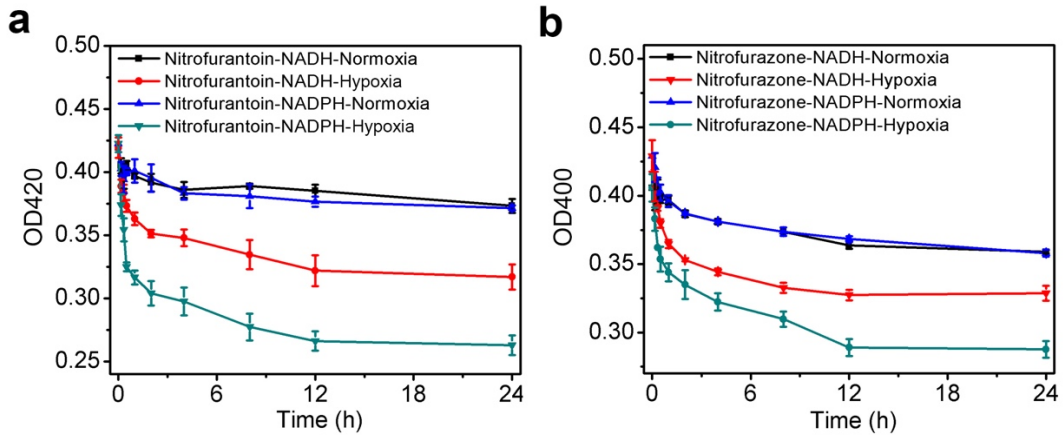


**Supplementary Fig. 7** Characterization of nitroreductase activity from MRSA under different conditions. **a,b,** Absorbance of nitrofurantoin (**a**) and nitrofurazone (**b**) at 420 nm (OD420) and 400 nm (OD400), respectively, after incubated with cell extracts of MRSA biofilms in normoxic condition and hypoxic condition (5% $O_2$, 95% $CO_2$) for different times (n = 3 biologically independent samples; mean ± SD). Source data are provided as a Source Data file.

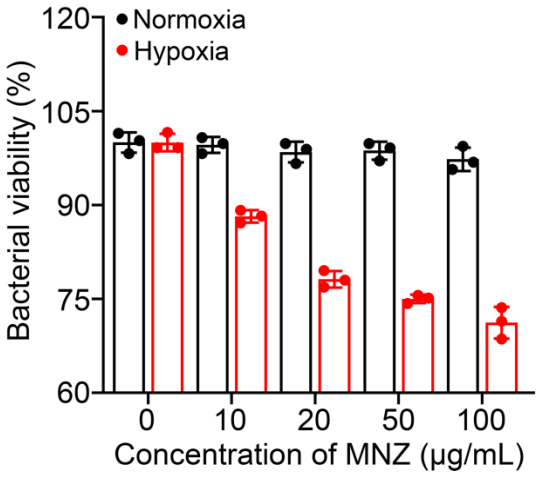


**Supplementary Fig. 8** Bacterial viability of MRSA after incubated with MNZ for 12 h under normoxic condition and hypoxic (5% $O_2$, 95% $CO_2$) condition (n = 3 biologically independent samples; mean ± SD). Source data are provided as a Source Data file.

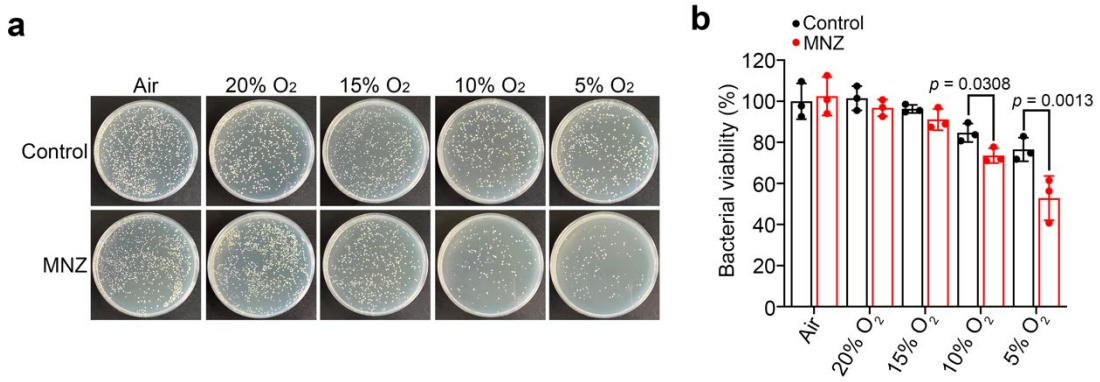


**Supplementary Fig. 9** Bacterial inactivation efficiency of MNZ under different $O_2$ levels. **a,** Photographs of the MRSA colony grown on LB plates after incubated without or with MNZ (50 μg/mL) for 24 h under different $O_2$ levels. **b,** Bacterial viability of MRSA after incubated without or with MNZ (50 μg/mL) under different $O_2$ levels (n = 3 biologically independent samples; mean ± SD). Statistical significance was analyzed via two-way ANOVA with a Tukey post-hoc test. Source data are provided as a Source Data file.

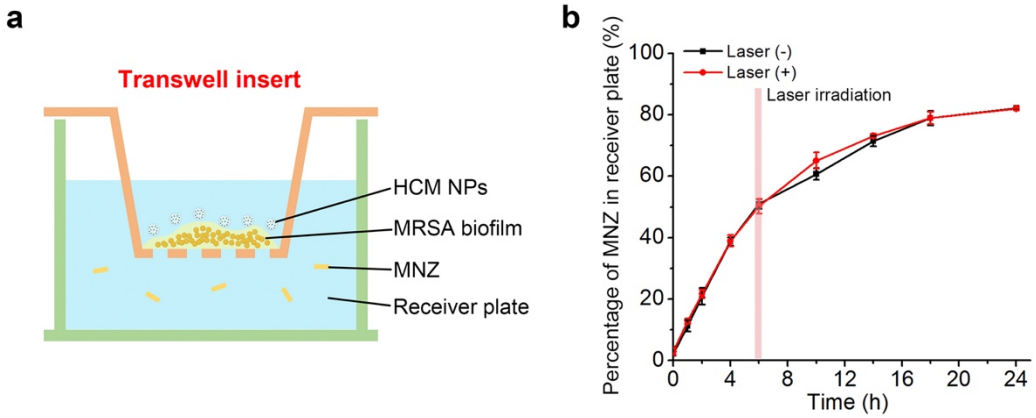


**Supplementary Fig. 10** Penetration of MNZ within MRSA biofilms. **a,** Schematic illustration for the penetration of MNZ in MRSA biofilms grown on Transwell inserts after incubation with HCM NPs. **b,** Percentage of MNZ from HCM NPs penetrated within MRSA biofilms with or without laser irradiation (635 nm, 20 mW/cm$^2$, 30 min) for different times (n = 3 biologically independent samples; mean ± SD). Source data are provided as a Source Data file.

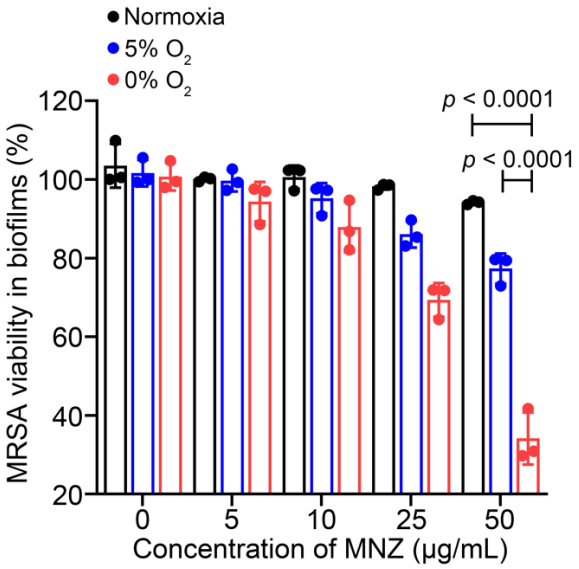


**Supplementary Fig. 11** Viability of MRSA in biofilms after incubated with different concentrations of MNZ under different $O_2$ levels (n = 3 biologically independent samples; mean ± SD). Statistical significance was analyzed via two-way ANOVA with a Tukey post-hoc test. Source data are provided as a Source Data file.

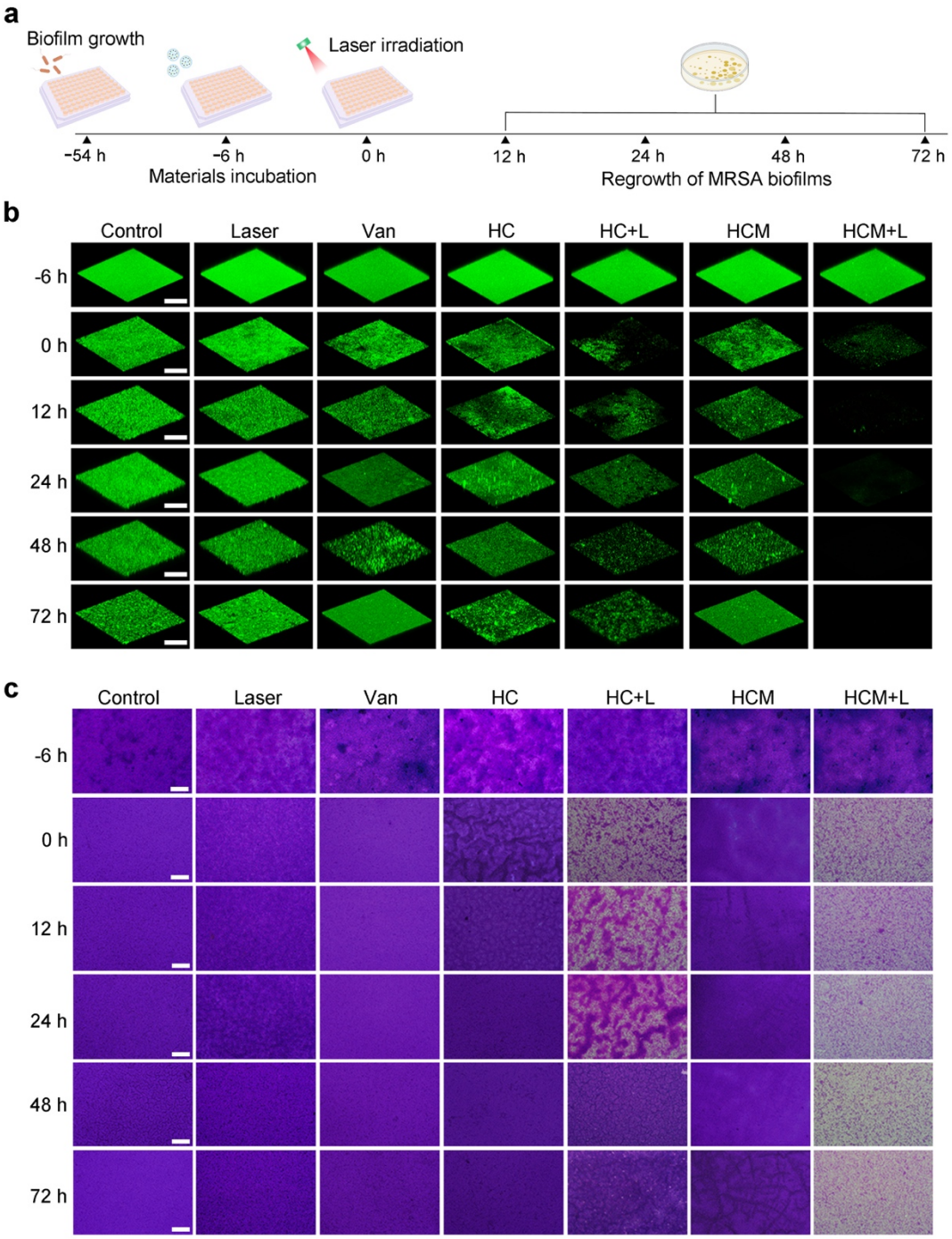


**Supplementary Fig. 12** Long-term inhibition of MRSA biofilms treated by HCM NPs *in vitro*. **a,** Schematic illustration of the experimental procedure. **b,** 3D CLSM images of MRSA biofilms stained by Calcein-AM (green) after various treatments. Scale bar is 200 μm. The size of CLSM images is 630 μm × 630 μm. **c,** Micrographs of MRSA biofilms stained by crystal violet after various treatments. Scale bar is 200 μm. Three independent experiments were performed and representative results are shown in **b** and **c**.

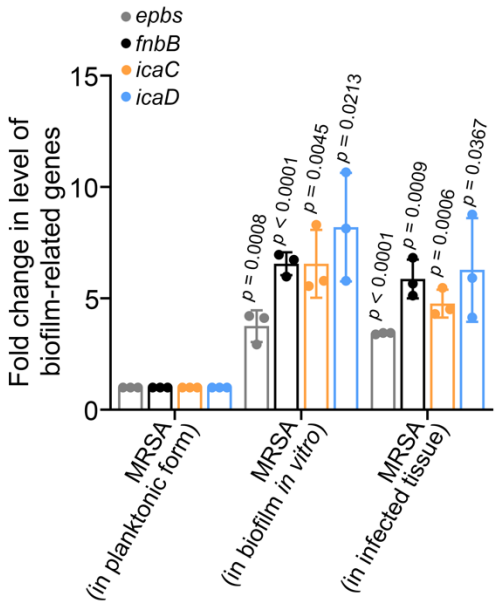


**Supplementary Fig. 13** Expression levels of *ebps*, *fnbB*, *icaC*, and *icaD* transcripts from MRSA in biofilm *in vitro* and infected tissues versus planktonic MRSA (n = 3 biologically independent samples; mean ± SD). Statistical significance was analyzed via two-way ANOVA with a Tukey post-hoc test. Source data are provided as a Source Data file.

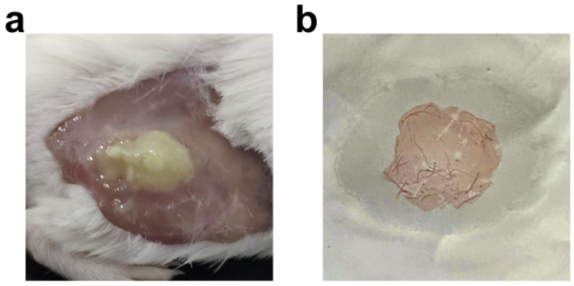


**Supplementary Fig. 14** Biofilm detection by using wound blotting method. **a,b,** Photographs of MRSA biofilm infected tissue (**a**) and ruthenium red stained nitrocellulose membrane (**b**) applied with infected tissue.

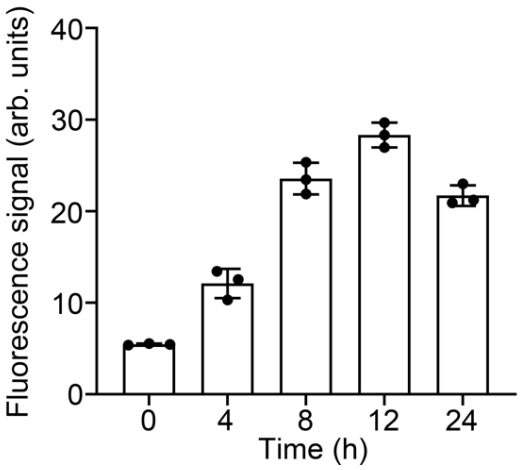


**Supplementary Fig. 15** The average fluorescence signal of MRSA biofilm infected sites after mice *i.v.* injected with HCM NPs for different times (n = 3 biologically independent samples; mean ± SD). Source data are provided as a Source Data file.

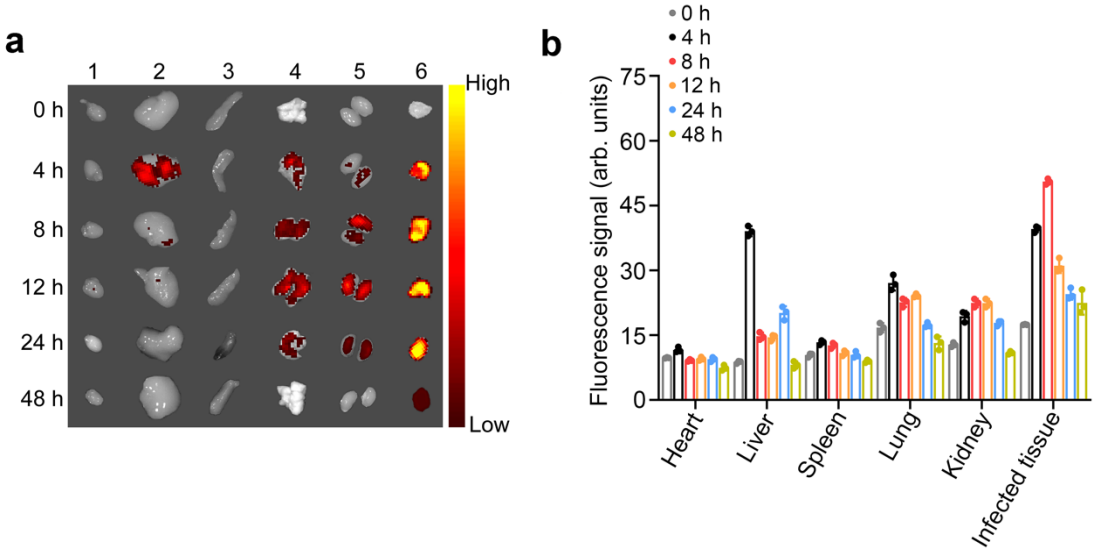


**Supplementary Fig. 16** Retention and distribution of HCM NPs in MRSA biofilm infected mice after *i.v.* injection. **a,b,** Fluorescence images (**a**) and average fluorescence intensity (**b**) of mice major organs (heart (1), liver (2), spleen (3), lung (4), kidney (5)) and biofilm infected tissues (6) after *i.v.* injection of HCM NPs (Ce6 = 4 mg/kg; MNZ = 2 mg/kg) at different times (n = 3 biologically independent samples; mean ± SD). Source data are provided as a Source Data file.

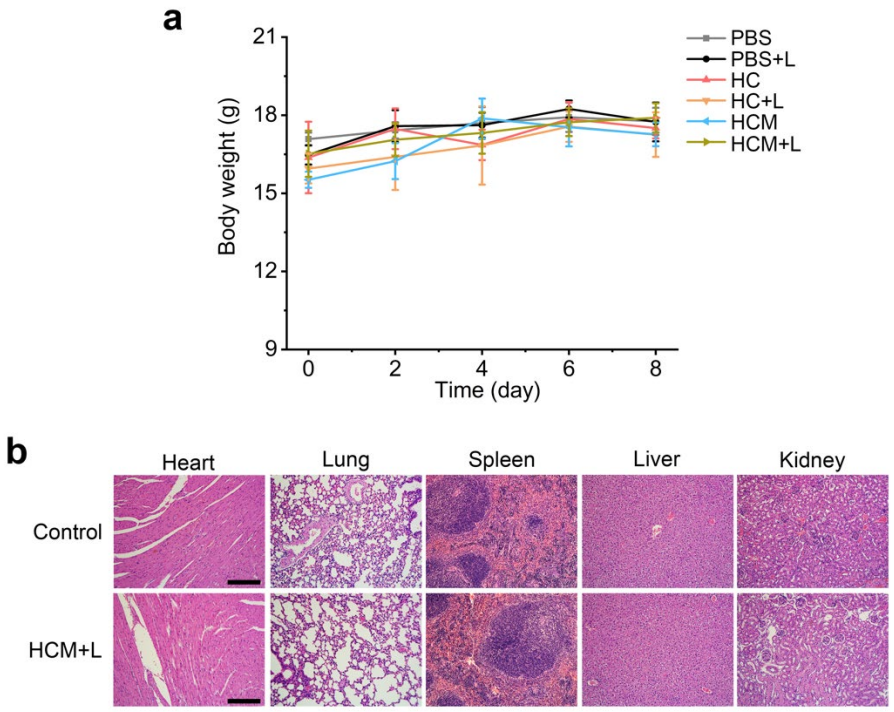


**Supplementary Fig. 17** Toxicity evaluation of HCM NPs to MRSA biofilm infected mice with laser irradiation. **a,** Body weights of the mice after various treatments (n = 5 biologically independent animals; mean ± SD). **b,** Micrographs of H&E stained slices of major organs (heart, liver, spleen, lung, and kidney) of mice after treatments with PBS (Control) and HCM NPs with laser irradiation (HCM+L) at 8 d post-treatment. Scale bar is 200 μm. Source data are provided as a Source Data file.

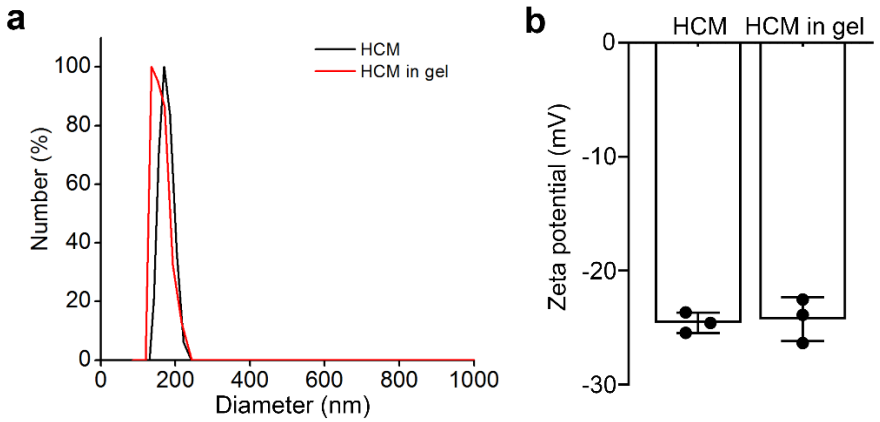


**Supplementary Fig. 18** Hydrodynamic sizes and zeta potential of HCM NPs at different conditions. **a,b,** Hydrodynamic sizes (**a**) and zeta potential (**b**) of free HCM NPs and HCM NPs in sprayed gel (n = 3 independent samples; mean ± SD). Source data are provided as a Source Data file.

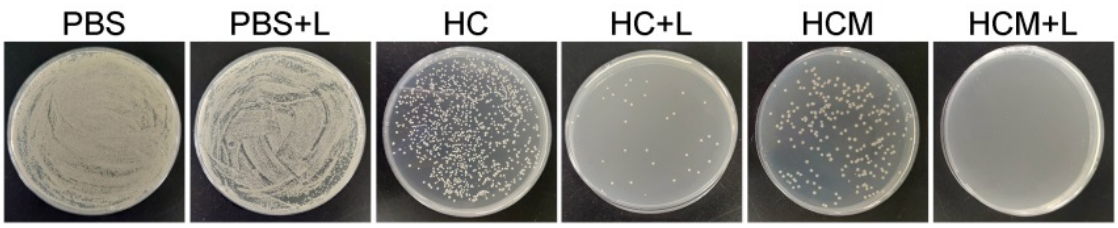


**Supplementary Fig. 19** Photographs of the MRSA colony grown on LB plates from PBS dispersions of biofilm infected tissues at 12 d post-treatment.

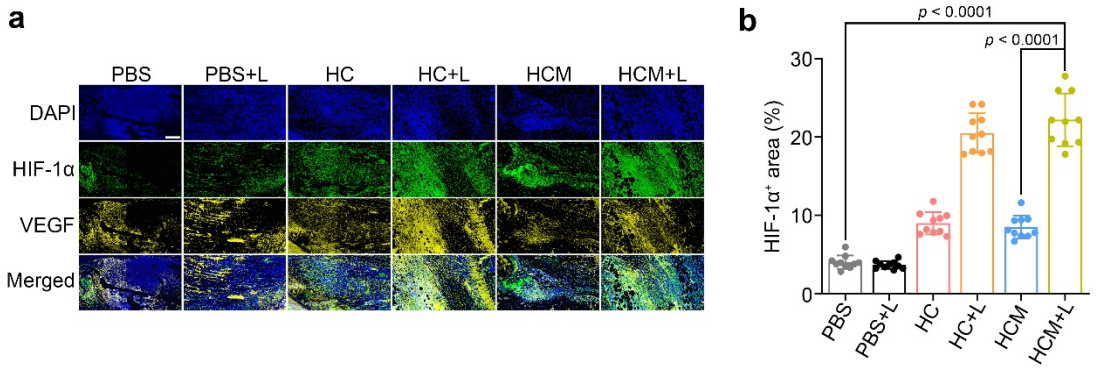


**Supplementary Fig. 20** Hypoxic condition of MRSA biofilm infected wounds in diabetic mice. **a,** Immunofluorescence images of HIF-1α (green) and VEGF (yellow) in infected wounds at 4 d post-treatment. **b,** Percentage of HIF-1$\alpha^+$ area in immunofluorescence images (n = 10 biologically independent samples; mean ± SD). Scale bar is 200 μm. Statistical significance was analyzed via one-way ANOVA with a Tukey post-hoc test. Source data are provided as a Source Data file.

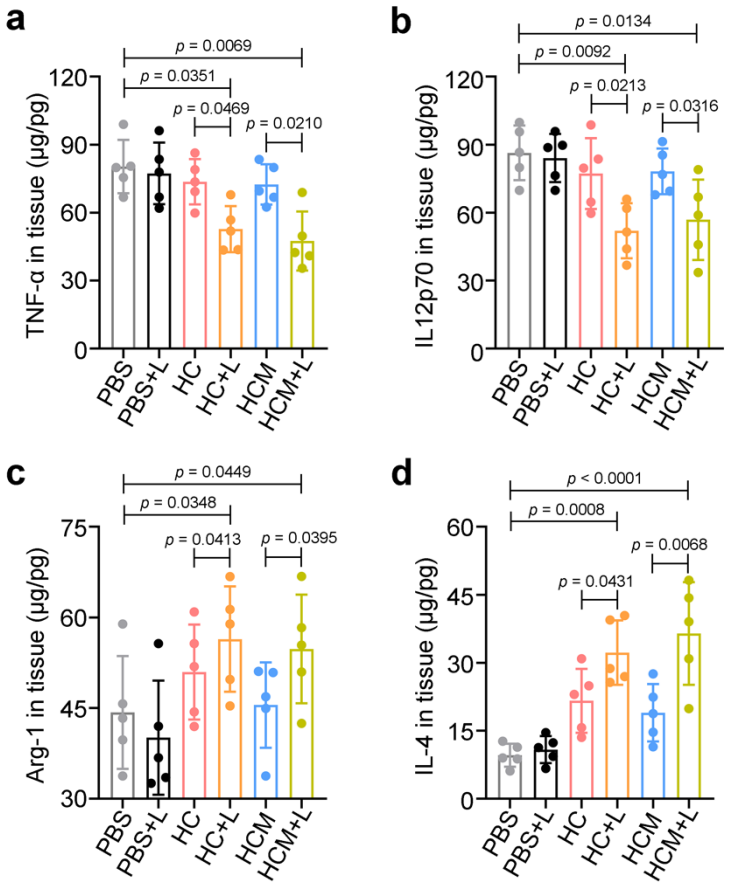


**Supplementary Fig. 21** Secretion levels of TNF-α (**a**), IL-12p70 (**b**), Arg-1 (**c**), and IL-4 (**d**) in infected tissues at 4 d post-treatment (n = 5 biologically independent samples; mean ± SD). Statistical significance was analyzed via one-way ANOVA with a Tukey post-hoc test. Source data are provided as a Source Data file.

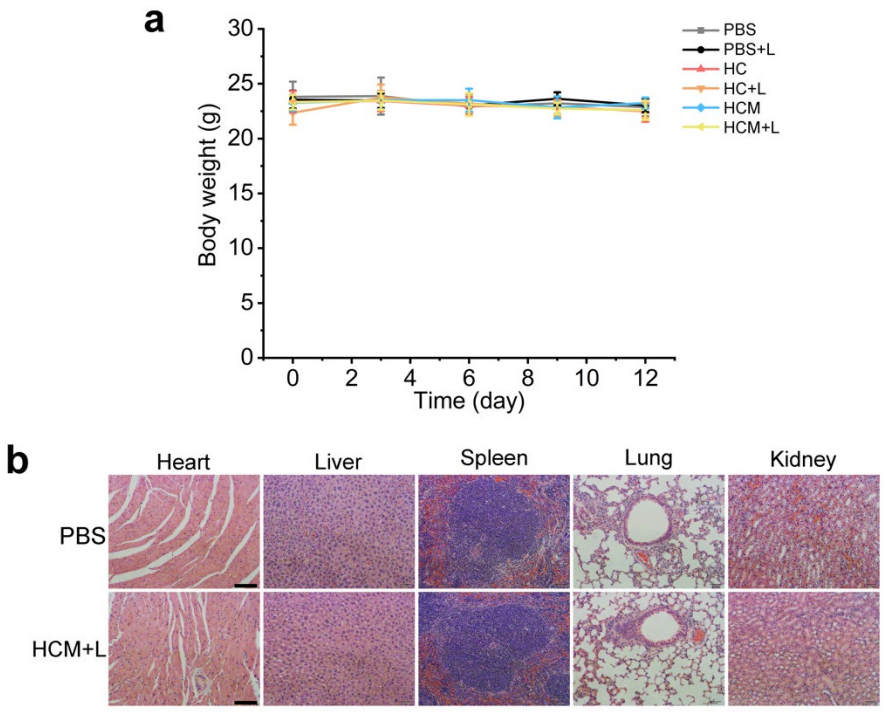


**Supplementary Fig. 22** Toxicity evaluation of the HCM gel to biofilm infected diabetic mice. **a,** Body weights of the mice at 12 d post-treatment (n = 5 biologically independent animals; mean ± SD). **b,** Micrographs of H&E stained slices of major organs (heart, liver, spleen, lung, and kidney) after treatments with PBS (Control) and HCM NPs with laser irradiation (HCM+L) at 12 d post-treatment. Scale bar is 100 μm. Source data are provided as a Source Data file.

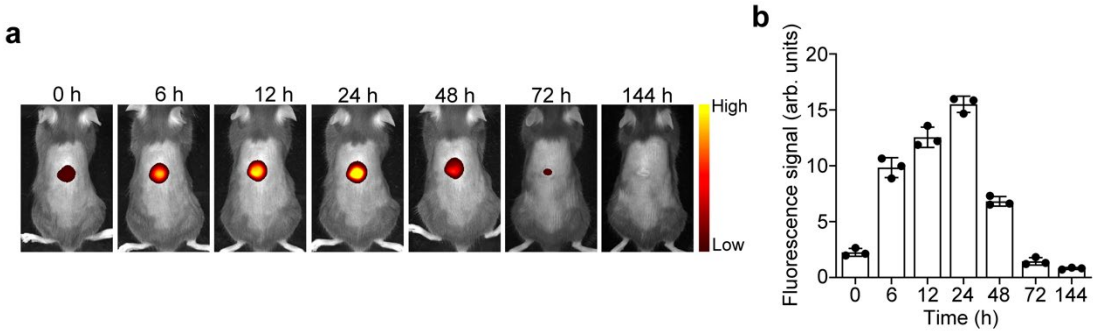


**Supplementary Fig. 23** Fluorescence imaging of biofilm infected wound in mice after treated with HCM gel. **a,b,** Fluorescence images (**a**) and fluorescence intensity (**b**) of biofilm infected wound in mice after treated with HCM gel for different times (n = 3 biologically independent animals; mean ± SD). Source data are provided as a Source Data file.

**Supplementary Table 1** Sequences of oligonucleotide primers used for qPCR[2].

| Genes | Nucleotide sequence of primers (5'-3') | Accession numbers | Annealing temperature | Amplicon size (bp) |
|---|---|---|---|---|
| ***epbs*** | 5-GGTGCAGCTGGTGCAATGGGTGT-3<br>5-GCTGCGCCTCCAGCCAAACCT-3 | U48826.2 | 60°C | 191 |
| ***fnbB*** | 5-ACGCTCAAGGCGACGGCAAAG-3<br>5-ACCTTCTGCATGACCTTCTGCACCT-3 | X62992.1 | 60°C | 197 |
| ***icaC*** | 5-CTTGGGTATTTGCACGCATT-3<br>5-GCAATATCATGCCGACACCT-3 | AF086783 | 60°C | 209 |
| ***icaD*** | 5-ACCCAACGCTAAAATCATCG-3<br>5-GCGAAAATGCCCATAGTTTC-3 | AF086783 | 60°C | 211 |
| **16sRNA** | 5-GGGACCCGCACAAGCGGTGG-3<br>5-GGGTTGCGCTCGTTGCGGGA-3 | L37597.1 | 60°C | 191 |

**Supplementary References**

1. Hussain, M., Hastings, J. & White, P. A chemically defined medium for slime production by coagulase-negative staphylococci. *J. Med. Microbiol.* **34**, 143 (1991).

2. Atshan, SS. et al. Quantitative PCR analysis of genes expressed during biofilm development of methicillin resistant *Staphylococcus aureus* (MRSA). *Infect., Genet. Evol.* **18**, 106-112 (2013).

3. Nakagami, G. et al. Biofilm detection by wound blotting can predict slough development in pressure ulcers: A prospective observational study. *Wound Repair Regen.* **25**, 131-138 (2017).